Soft Computing (2025) 29:4673–4684
https://doi.org/10.1007/s00500-025-10676-y

APPLICATION OF SOFT COMPUTING

# Efficient thermal comfort estimation employing the C-Mantec constructive neural network model

Francisco Ortega-Zamorano[1] · José M. Jerez[1] · José Rodríguez-Alabarce[1] · Kusha Goreishi[1,2] · Leonardo Franco[1]

Accepted: 3 May 2025 / Published online: 26 July 2025


**Abstract**
Thermal comfort is the condition in which a person feels satisfaction with the thermal environment through a subjective evaluation. In this work, a compact and efficient estimation of thermal comfort perception by human subjects is performed using a constructive neurocomputational model trained with data generated in controlled conditions with 49 volunteers giving 705 different scenarios, allowing, thanks to the versatility of the model, an interpretable and simple resulting function facilitating an easy handling of the results by people from different fields. The results have been compared with two of the most used standard methods for modelling thermal comfort: Fanger and COMFA models, and they show an improvement in terms of accuracy and mean square error both in a binary decision scenario (comfort or not) as well as for a discrete decision-making case in which different thermal comfort regions are considered. The flexibility of the neural model permits the incorporation of extra subject-related variables that increases further the thermal comfort estimation and, also, permits the implementation of the model in distributed and low cost/low consumption systems.

**Keywords** Supervised learning · Constructive neural networks · Thermal comfort · BMI

## 1 Introduction

Thermal comfort describes the condition of the mind in which satisfaction with the thermal environment is expressed. To achieve this satisfaction, the first condition is "thermal neutrality", that is, that the person feels neither too hot nor too cold. Computing thermal comfort is challenging because the value involves a subjective sensation, which varies from person to person and their activities (work, relax, sports activities, etc.) and, also, on the measurement of the environment variables such as temperature, humidity and wind speed. Issues regarding thermal comfort and its applications have been tackled by different point of view: building scientists Alghamdi et al. (2022), urban planners Liu et al. (2023), social scientists Lopez and Heard (2023), anthropologists Feng et al. (2023) and Heating, Ventilating and Air Conditioning (HVAC) design engineers (Acquaah et al. 2023; Ono et al. 2022) including systems to predict demands for the heating and cooling in cars Chen et al. (2024) among other professions, and have recently attracted the attention of climate researchers in relationship to climate change issues (Pallubinsky et al. 2023; Nam et al. 2024).

Through the history, different civilizations have taken into account thermal comfort in living design in order to isolate and control the thermal and humidity qualities of a space. However it was not until the twentieth century that studies were conducted to provide the basis for modelling thermal comfort. Povl Ole Fanger made a breakthrough in 1970, laying the groundwork for theoretically modelling thermal comfort based on the imbalance between the actual heat flow from the body in a given thermal environment and the heat flow required for optimum comfort (i.e., neutral) for a given activity. Fanger devised a "comfort equation" mixing ambient parameters (i.e., humidity level, air velocity, mean radiant temperature and air temperature) in which, for a specific grade of activity and type clothing, the highest proportion of people are likely to be comfortable Fanger (1967). He proposed a related index, named the Predicted Percentage Dissatisfied (PPD), which is computed from Predicted Mean Vote (PMV), in order to measure the quality of

✉ Francisco Ortega-Zamorano
pacoortega@uma.es

[1] Department of Computer Science, E.T.S.I. Informática, University of Málaga, Bulevar Louis Pasteur, 35, 29071 Málaga, Spain

[2] Quark Arquitecs, Benalmádena, Spain

indoor environments and to evaluate the level of discomfort of the inhabitant. The PMV-PPD method, based on Fanger theory, has been applied to define comfort zones in international standards such as the ISO 730:2005 norm, which establishes the requirements for general thermal comfort and local thermal discomfort Olesen and Parsons (2002) and the ASHRAE Standard 55 that specifies the ranges of indoor environmental conditions to achieve acceptable thermal comfort for building occupants Ashrae (2010).

Urban planning and efficient architecture are very relevant issues in recent years due to people's awareness of personal welfare associated with thermal comfort Lindberg et al. (2018). In outdoor spaces the solar radiation is a factor affecting thermal comfort, being in many occasions the most relevant variable, but nevertheless the Fanger method does not take into account for this component. Later studies did introduce this factor and for example a model named COMFA has been proposed by Brown and Gillespie Brown and Gillespie (1986) in 1986 in which this factor becomes relevant. Posterior works also consider the inclusion of wind and activity effect on the clothing microclimate for building an outdoor thermal comfort model aimed for subjects performing physical activity (Kenny et al. 2009a, b).

The Fanger and COMFA models are typically used through simple computer programs that, given a specific set of conditions, provide an estimate of perceived thermal comfort. Artificial Neural Networks (ANNs) Iman et al. (2023), Ganaie et al. (2022) are systems inspired by how the human brain works, though not identical, and are often used for classification and clustering tasks. They have been applied successfully in many areas, such as industrial processes, stock market analysis, pattern recognition, medical diagnosis, and control systems (Zadmirzaei et al. 2024; Pilliza et al. 2018; Bindu and Sastry 2023; Torres-Molina et al. 2020).

Neural networks have evolved significantly since their inception, taking a great leap in recent years largely, since the emergence of deep learning models LeCun et al. (2015) that have shown higher performance compared to the Backpropagation algorithms traditionally used for prediction problems. In addition, the emergence not only of these new network structures but also of new transfer functions (Kisel'ak et al. 2021; López-Rubio et al. 2019), that improve performance have made neural networks one of the most widely used techniques in the field of computer science. However, this growth has created increasingly complex systems that need a large amount of processing capacity, requiring specific hardware sometimes costly and sensible to parameter tuning, making it impossible to implement in general distributed or standard real-time systems. Furthermore, the resulting prediction functions are not easily interpretable, giving rise to prediction black boxes that are difficult to use by people outside the field of computing.

In recent years, neurocomputational models have been widely used to estimate thermal comfort in various contexts. This includes their application in optimizing heating, ventilation, and air conditioning (HVAC) systems (Ferreira et al. 2012; Castilla et al. 2013), predicting physiological variables such as core and local skin temperatures Michael et al. (2017), and modeling the distribution of solar spectral irradiance Moreno-Sáez and Mora-López (2014).

However, these works have shown methods that improve over traditional ones, they still have a high computational cost, making them difficult to implement in distributed systems with a resulting non-interpretable function.

Ortega-Zamorano et al. (2014) implemented an expert system in a low-cost microcontroller which consisted of an intelligent sensor/actuator that measures five environmental variables and takes a decision taking into account previous events through an artificial neural network, achieving a distributed system where the learning process is done on the device itself quickly and inexpensively.

Also, Rodríguez-Alabarce et al. (2016) introduced a neurocomputational model to estimate the thermal comfort in order to define the main factors in the equation and how the temperature influences in the thermal comfort model.

In this paper, we implement a neurocomputational thermal comfort model using data collected from 49 volunteers exposed to different conditions, to obtain a model tested in real life. Artificial neural networks implemented through the C-Mantec constructive neural network algorithm Subirats et al. (2012) have been utilized for the estimation of the subjective thermal comfort, allowing, thanks to the versatility of the model, an interpretable and very simple resulting function that facilitates easy handling of the resulting system by people from all fields of science. Also adding new subject-related variables to the prediction process for comparing the predicted values with those perceived by the subjects and to the prediction obtained from Fanger and COMFA models, in order to obtain an improvement in the calculation of the prediction Comfort.

The work is structured as follows: first, we describe in Section 2 Fanger and COMFA models, followed by a description of the C-Mantec constructive neural network algorithm in Section 3. Section 4 gives details of the data collection process and equipment used, together with a descriptive analysis of the data. Thereafter, the predictions obtained by the three models are analyzed and discussed in Section 5, to finally extract conclusions in Section 6.

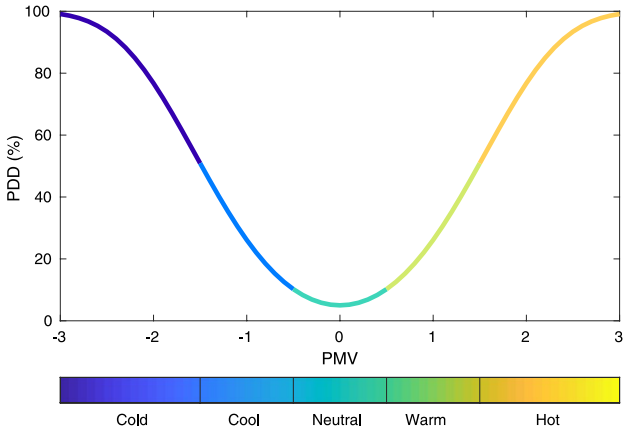


**Fig. 1** Predicted Percentage of Dissatisfied (PPD) people from a group in relationship to the PMV value in the range [− 3,3]

**Table 1** Thermal comfort in relationship to the energy balance obtained from the COMFA scale

| Balance (B) | Sensation |
|---|---|
| 150 < B | Very Hot |
| 50< B< 150 < | Hot |
| − 50 < B < 50 < | Comfort |
| − 150 < B < − 50 < | Cold |
| B< − 150 < | Very Cold |

## 2 Theoretical models of the thermal comfort

### 2.1 The fanger model

The Fanger model of thermal comfort is a heat balance model that evaluates thermal comfort by considering physiological and environmental factors. It is based on the principle that the body regulates its temperature to maintain thermal equilibrium, where heat production matches heat loss.

Body thermoregulated activity includes natural mechanisms like sweating or shivering to stabilize internal temperature. In thermal equilibrium, these efforts are minimal, reducing strain and ensuring comfort. The Fanger model predicts and optimizes conditions to achieve this state.

The method represents the mean thermal sensation vote on a standard scale, called Predicted Mean Vote (PMV), that permits to estimate an index named predicted percentage of dissatisfied (PPD) people that can be determined for that particular environment conditions by means of the equation:

$$PDD = 100 - 95 \cdot e^{(-0.03353 \cdot PMV^4 - 0.2179 \cdot PMV^2)} \quad (1)$$

During his research, two different mechanisms were observed by Fanger which are relevant in thermal comfort, the sudoration (sweating) and skin mean temperature, which are dependent on the physical activity of the person in which thermal comfort is determined. A similar relationship exists for the skin mean temperature, remarking that skin temperature decreases as the physical activity increases. From these two relationships, Fanger proposed a heat balance equation from which a thermal neutrality condition can be obtained, taking into account factors as metabolic rate, clothing insulation, air temperature and speed, mean radiation temperature and relative humidity. The PMV equation described by Fanger states that:

$$PMV = (0.303 \cdot e^{(-0.36 \cdot M_a)} + 0.028) \cdot (M_a - A - B - C - D - E - F) \quad (2)$$

where $M_a$ is the metabolic rate and A, B, C, D, E, F are heat losses by diffusion through the skin, by sweating, latent breathing, dry by breath, by radiation, and by convection respectively.

Figure 1 shows the relationship between the predicted percentage of dissatisfied (PPD) people from a group in relationship to PMV values ranging from − 3 to 3.

PMV values are widely used for setting international ergonomic ambient standards in indoor spaces (ANSI/AHSRAE 55 and ISO 7730) and have also been used for tuning self-regulated cooling-heating systems HVAC4.

### 2.2 The COMFA model

Due to the fact that the Fanger model does not take into account surrounding and solar radiation, this model has been employed in indoor environments, giving accuracy problems when is used in outdoor environments. In order to model these tasks, an equation was introduced in 1986 by Robert Brown and Terry Gillespie for the estimation of thermal comfort known as COMFA method Brown and Gillespie (1986) in which the solar radiation is taking into account.

The COMFA models compare the relationship of energy balance between a person and the ambient, introducing the coefficient of energy balance between absorbed surrounding and solar radiation which allows its use in outdoor areas. According to the COMFA method the energy balance can be calculated as:

$$Balance = M + R - E - C - L\,, \quad (3)$$

where $M$ is the metabolic heat, $R$ is the absorbed surrounding and solar radiation, $E$ is the evaporation energy, $C$ refers to convective energy and $L$ is the emitted radiation.

All sources of heat are expressed in $W/m^2$, and so is the final balance relationship. The energy balance can then be related to thermal comfort sensation using the relationship shown in Table 1.

The COMFA model has undergone some modifications by adjusting the parameters that relates the factors with the

estimated value, in order to develop several new models from the original model. We have used the most realistic COMFA model in outdoor environments to compare with our proposed system to obtain a fair comparison Sangkertadi and Syafriny (2014).

## 3 Artificial neural network models and the C-Mantec algorithm

Artificial neural network models are mathematical models inspired in the functioning of the brain that can be used for clustering and classification tasks (Haykin 1998; Mehrotra et al. 1997; Reed and Marks 1998). Several neural network models have been developed in the past, but in particular for classification tasks the most used architectures are those using a feed-forward processing of the information. Among them, multilayer perceptrons trained by the back-propagation algorithm or the more recent Deep Learning architectures, are the most popular methods. However, in almost all cases, choosing a particular neural architecture for a given problem is a complex and time-consuming task, and thus alternative models have been proposed that automatically build the architecture Franco et al. (2010). C-Mantec Subirats et al. (2012) (Competitive Majority Network Trained by Error Correction) is a constructive neural network algorithm designed to automatically build compact single-hidden-layer architectures with strong predictive performance for supervised classification tasks. Unlike traditional approaches, C-Mantec constructs the network topology dynamically during the training process, as input patterns are presented, thus eliminating the need to predefine the architecture. A key innovation of C-Mantec compared to earlier constructive models is that its hidden layer neurons compete to learn the data using a modified perceptron learning rule known as the thermal perceptron Frean (1990), which has been shown to produce highly compact architectures Gómez et al. (2020).

The classification/prediction process for a neural network or any other alternative model generally involves at least two phases: training, where the internal parameters of the model (the synaptic weights connecting the neurons) are adjusted according to the training data, and the test phase in which the performance of the model is evaluated on data not previously used in the training phase. C-Mantec generates during the training phase feed-forward neural network architectures that includes an input layer of non-processing units that only have the function to insert the pattern information into the system, a single hidden layer of binary units, and an output layer with a single neuron that computes the majority function according to the activation of the neurons in the previous layer. In the test phase, the synaptic weights are kept fixed, and the test pattern responses output by the network are compared to their real category, essentially analyzing whether the network correctly predicts or not the category label of the test patterns. In Fig. 6, an architecture created using C-Mantec is shown for the problem of estimating thermal comfort. The functioning of the C-Mantec architecture is as follows: the binary activation state (S) of the neurons in the hidden layer depends on the $N$ input signals coming from the input layer, $\psi_i$, and on the actual value of the $N$ synaptic weights ($\omega_i$) and bias ($b$), which connects the input layer with the hidden neurons:

$$S = \begin{cases} 1 & \text{if } h \geq 0 \\ 0 & \text{otherwise} \end{cases} \tag{4}$$

where $h$ represents the synaptic potential of a hidden neuron, defined as:

$$h = \sum_{i=0}^{N} \omega_i \, \psi_i \tag{5}$$

According to the thermal perceptron rule, the synaptic weights $\Delta\omega_i$ are updated on-line, immediately after presenting a single input pattern, following the equation:

$$\Delta\omega_i = (t - S) \, \psi_i \, T_{fac}, \tag{6}$$

where $t$ is the target value of the input presented, and $\psi$ denotes the input value of the unit $i$, which is connected to the output through the weight $\omega_i$. A distinctive aspect of the thermal perceptron compared to the standard perceptron learning rule is the inclusion of the $T_{fac}$ factor, which is calculated as shown in Eq. 7 as a function of the synaptic potential and a temperature parameter (T) that is introduced artificially during learning.

$$T_{fac} = \frac{T}{T_0} e^{-\frac{|h|}{T}}, \tag{7}$$

The value of $T$ decreases as the learning process is carried out, according to Eq. 8, following a gradual temperature reduction strategy.

$$T = T_0 \cdot (1 - \frac{I}{I_{max}}), \tag{8}$$

where $I$ denotes the index of the current iteration within a learning cycle, and $I_{max}$ sets the upper limit on the total number of iterations allowed during the training process. A learning cycle begins when a randomly selected pattern is presented to the network and ends when the network output matches the target of that pattern, or when a selected neuron

(either the one with the highest $T_{fac}$ value or a newly added one) updates its synaptic weights to learn the presented input.

The C-Mantec algorithm requires three parameters to be set at the beginning of the learning process. Various experiments have demonstrated its robustness, showing that it performs reliably across a wide range of parameter values. These parameters are the following:

- $I_{max}$: maximum number of learning iterations allowed for each neuron in one learning cycle.
- $g_{fac}$: growing factor that determines when to stop a learning cycle and include a new neuron in the hidden layer.
- $\phi$: determines in which case an input example is considered as noise and removed from the training dataset according to the following condition:

$$\text{delete}(x_i) \mid N_{LT} \geq (\mu + \phi\, \sigma), \tag{9}$$

where $x_i$ represents an input pattern, $N$ is the total number of patterns in the data set, $N_{LT}$ is the number of times that pattern $x_i$ has been presented to the network in the current learning cycle, and where $\mu$ and $\sigma$ correspond to the mean and variance of the distribution for all patterns on the number of times that the algorithm has tried to learn each pattern in a learning cycle. The learning procedure starts with one neuron present in the single hidden layer of the architecture and an output neuron that computes the majority function of the responses of the hidden neurons (a voting scheme). The process continues by presenting an input pattern to the network and if it is misclassified, it will be learned by one of the present neurons whose output did not match the target pattern value if certain conditions are met, otherwise a new neuron will be included in the architecture to learn it. Among all neurons that misclassified the input pattern, the one with the largest $T_{fac}$ will learn it but only if this $T_{fac}$ value is larger than the $g_{fac}$ parameter of the algorithm, a condition included to prevent the unlearning of previous stored information. If no thermal perceptron meeting these criteria is found, a new neuron is added to the network, starting a new learning cycle that includes the resetting of all neurons temperature to $T_0$. Also at the end of a cycle the noisy patterns filtering procedure (Eq. 9) is applied. The algorithm continues its operation iteratively repeating the previous stages until all patterns in the training set are correctly classified by the network. During the learning process catastrophic forgetting is prevented as synaptic weights are only modified if the change involved is small (controlled by the value of $g_{fac}$ and by an annealing process that reduces the temperature as learning proceeds), as if this is not the case, the algorithm introduces a new neuron in the architecture.

The work that explains in detail the design of the C-Mantec algorithm Subirats et al. (2012)shows how the algorithm is very stable in reference to the parameters to be set at the time of starting the learning procedure. This work describes in detail the selection of parameters, and these parameters must be within the following ranges:

- $g_{fac} \in \{0.05 - 0.5\}$.
- $I_{max} \in \{1000 - 100000\}$.
- $\phi \in \{1 - 3\}$.

Although the algorithm has proven to have very little variability when the parameters are changed, a series of runs with different settings have been launched. The different configurations have been $g_{fac} = \{0.1, 0.2, 0.3, 0.4, 0.5\}$, $I_{max} = \{1000, 5000, 10000, 20000\}$and$\phi = \{1, 2, 3\}$resulting in results without statistical difference. The parameters that we have finally selected, because it is the configuration that provides the best efficiency values between classification measures and computing time, have been: $g_{fac} = 0.5.$, $I_{max} = 10000.$, $\phi = 2$.

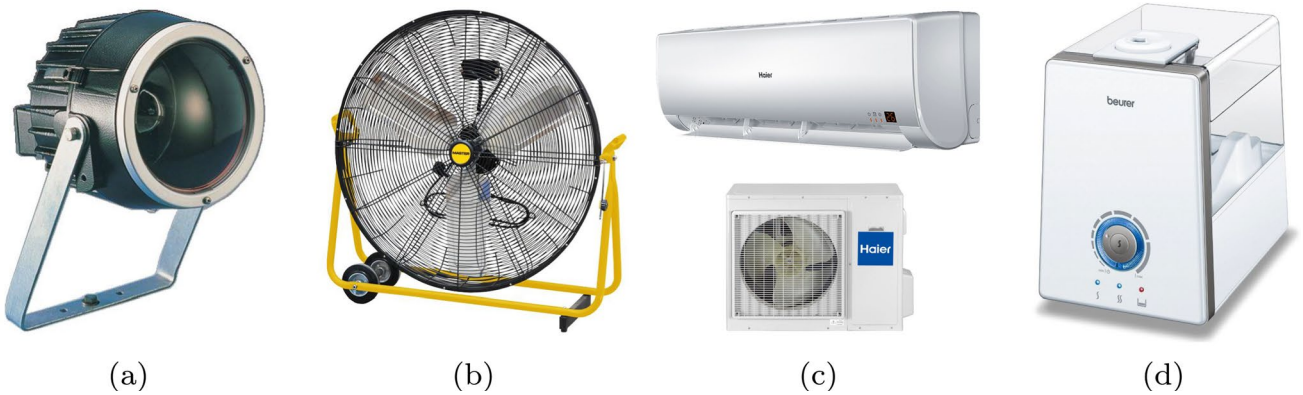


**Fig. 2** Devices used to control the environmental variables, (**a**) CSI-OQ-1000 Thorn lamp (radiation), (**b**) Industrial fan mf-30p (wind), (**c**) Haier Brezza-12K HVAC system (temperature and humidity), and (**d**) humidifier Beurer LB-88 ( humidity)

**Table 2** Characteristics of elements used to control the environmental variables, (a) irradiance levels control device, (b) wind condition control device, (c) the temperature sensation control device and (d) the humidity condition control device

| Characteristic | Value |
|---|---|
| **(a)** | |
| Dimension | (380 x 262 x 350) mm |
| Consumption | 1kW |
| Power | 1kW |
| Luminous Flux | 21500 lm |
| Color Temp. | 2900 K |
| **(b)** | |
| Dimension | (990 x 940 x 300) mm |
| Consumption | 378 kW |
| Max. airflow | 19.200 $m^3/h$ |
| Diameter | 750 mm |
| Rotation | 360° |
| **(c)** | |
| Dimension | (855 x 204 x 280) mm |
| Consumption | 1350 W |
| Cooling | 3600 W |
| Heating | 3700 W |
| Max. airflow | 650 $m^3/h$ |
| **(d)** | |
| Dimension | (295 x 195 x 280) mm |
| Consumption | 16-280 W |
| Capacity | 550 ml/h |
| Deposit | 6 l |

## 4 Experimental study with volunteers

For training and test the different thermal comfort models, a set of data is required, and thus a series of experiments with human subjects have been carried out. In order to do this and with the aim of testing different scenarios, a space was prepared in which the environmental variables are configured by the researchers using several devices (lamp, fan, air conditioner and humidifier) described below.

### 4.1 Control elements of environmental variables

The Fig.2a shows lamp CSI-OQ-1000 Thorn used to simulate different irradiance levels and different elevations and solar azimuth. The Fig.2b shows the industrial fans, mf-30 p, used to generate wind conditions with different speed levels. The Fig.2c shows the air conditioner Haier Brezza-12K installed in the space to cool or heat depending on the analyzed scenario for characterize. The Fig.2d shows the humidifier Beurer LB-88 employed in the regulation of the relative humidity of the air (Table 2 shows the main characteristics of the used devices.)

### 4.2 Measuring elements of environmental variables

Several devices have been used to measure the variables involved in the study of the thermal comfort. Fig.3a shows the environment meter PCE-EM882for measuring temperature and humidity. This device can also measure the light and the sound level but these functions were not used in this experiment. Fig.3b shows the portable Solarimeter Kimo SL 100 used to measure the solar radiant flow received by unit area. The Fig.3c shows the portable anemometer PCE-AM81 used to to measure wind speed. The main characteristics of these used devices are shown in Table 3.

### 4.3 Study group

Several tests carried out with the participation of 49 volunteers of different ages and body constitutions were performed in different environmental controlled conditions. Each person has been exposed to 15 experiments under variations of solar radiation, humidity, temperature, wind,


**Fig. 3** Devices used for measuring the variables involved in the study: (**a**) environment meter PCE-EM882 (temperature), (**b**) solarimeter Kimo SL 100 (irradiance level), (**c**) PCE-AM81 portable anemometer (wind speed)

clothing and activity in which values have been precisely monitored used the equipment described previously. Table 4 shows the range of values of the variables used in the experiments. The Body Mass Index (BMI) has been measured for all subjects as it can influence the thermal sensation. Blood Pressure (BP) was also measured during the experiments by means of the portable monitor "Beurer Medical BC32" but was not used for predicting thermal comfort. In the experiments the subjects have to indicate after a minimum of 120 seconds its comfort sensation in range of continuum values according to the ASHRAE scale.

A Principal Component Analysis (PCA) has been applied to the data obtained from the experiments. PCA is a statistical procedure that uses a linear orthogonal transformation to convert a set of observations of possibly correlated variables into a set of uncorrelated variables called principal components. The full set of principal components is as large as the original set of variables, but it is commonplace for the sum of the variances of the first few (two or three) principal components to exceed 80% of the total variance of the original data.

$$\underbrace{\begin{bmatrix} -5.36 & -82.60 & -106.74 & 19.51 & -24.04 & -25.39 & -10.70 & 54.16 & 63.26 & -95.61 \\ -12.11 & -4.95 & -102.50 & 30.44 & 14.18 & 16.59 & 0.32 & -45.36 & -8.57 & -72.64 \\ -37.75 & 5.66 & 40.18 & 40.85 & -38.69 & 1.46 & 12.34 & -56.11 & -21.56 & -41.63 \\ -23.93 & -3.73 & -45.19 & 1.98 & -4.33 & -44.83 & -5.53 & -9.30 & 4.94 & -86.32 \\ -17.06 & -13.52 & 11.42 & -23.47 & 5.53 & 29.82 & -9.06 & 9.73 & 8.78 & -4.86 \end{bmatrix}}_{M} \cdot \begin{bmatrix} X_1 \\ X_2 \\ X_3 \\ X_4 \\ X_5 \\ X_6 \\ X_7 \\ X_8 \\ X_9 \\ -1 \end{bmatrix} = \begin{bmatrix} Y_1 \\ Y_2 \\ Y_3 \\ Y_4 \\ Y_5 \end{bmatrix} \tag{10}$$

$$\text{Comfort} = [(Y_1 \geq 0) + (Y_2 \geq 0) + (Y_3 \geq 0) + (Y_4 \geq 0) + (Y_5 \geq 0)] \geq 5/2 \tag{11}$$

**Table 3** Characteristics of the devices used to measure the solar radiation (a), wind speed (b) and temperature and humidity (c)

| Characteristic | Value | Characteristic | Value | |
|---|---|---|---|---|
| **(a)** | | | | |
| Dimension | (50 x 120 x 33) mm | | | |
| Weight | 150g | | | |
| working temp. | $-10°C$+$50°C$ | | | |
| Range of measurement | 1-1300 $W/m^2$ | | | |
| Frequency of calculation | 2/s | | | |
| Accuracy | 5% mm | | | |
| **(b)** | | | | |
| Dimension | (156 x 60 x 33) mm | | | |
| Weight | 160g | | | |
| Range of measurement | 0.4...30.0 m/s | | | |
| Resolution | 0.1 m/s | | | |
| Accuracy | ±3%( < 20 m/s) | | | |
| | ±4%( >20 m/s) | | | |
| | | | Humid. | Temp. |
| **(c)** | | | | |
| Dimension | (251 x 64 x 40) mm | Range of measurement | 25-95 % H.r | − 20 +200 °C |
| | | Resolution | 0.1% | ± 3 % |
| Weight | 250g | Accuracy | ±5% | ± 3,5 % |

**Table 4** Set of standard and new variables and their range (or category) used for the estimation of thermal comfort sensation in the different experiments

| | Variable | Range/Categories |
|---|---|---|
| Standard | Radiation | $\{15, 250, 550, 850\} W/m^2$ |
| | Humidity | $[33 - 45]$ % |
| | Temperature | $[18 - 32]°C$ |
| | Wind | $[0 - 4] m/s$ |
| | Clothing | [Winter, Spring, Summer] |
| | Activity | [None, office type] |
| New | Age | $[22 - 50]$ Years |
| | Sex | $\{Male, Female\}$ |
| | BMI | $[19 - 34] Kg/m^2$ |

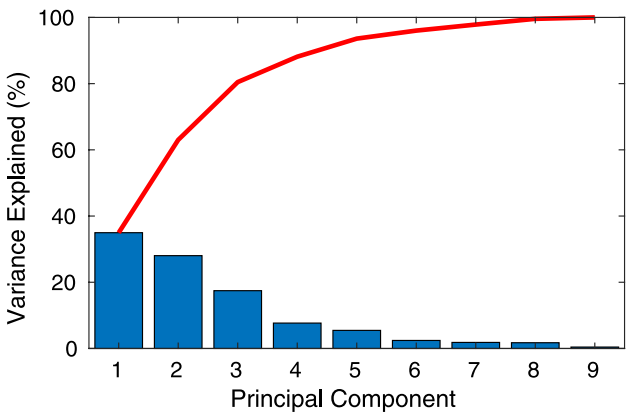


**Fig. 4** Percentage of variance explained by each of the principal components (vertical bars) and the accumulated value (solid line)

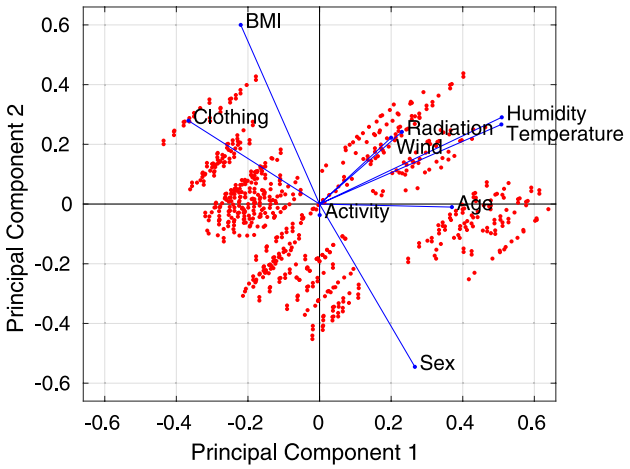


**Fig. 5** PCA representation of the data. All eight variables (solid lines) and recorded subject data (red dots) are represented in the bi-dimensional space of the first and second Principal Components

Fig. 4 shows the percentage of variance explained by each principal component (vertical bar) and the accumulated value of the previous components (solid line). The first two components explains approximately 60% of the total variance while using the three first components takes this level up to approximately 80%. Because 3-dimensional graphics are not well displayed in paper support document, we decided to perform an analyses of the subjects' data with only the 2 first components. Fig. 5 shows all nine experimental variables (subject and environmental conditions data), represented in this graph by a vector, which direction and length indicate how each variable contributes to the two principal components. The first principal component, on the horizontal axis, has positive coefficients for the majority of the variables, in particular for all of them except BMI and Clothing, being the largest coefficients corresponding to Humidity and Temperature. However, the second principal component, on the vertical axis, has positive coefficients for all variables except for the variable sex. The Activity variable, that can be hardly seen in the graph, contributes almost nothing to the two main principal components, and this is due to the fact that its contribution is related to the third component (not shown) that represents approximately 20 % of the total variance. The red dots in the figure represent the 705 observations recorded from the experiments as a function of the two principal components.

## 5 Results

One of the principal aims of this work is to test the prediction accuracy of a constructive neural network model (C-Mantec) regarding the thermal comfort sensation felt by subjects in different ambient conditions, and compare it to those that can be obtained from the Fanger and COMFA models.

In a first analysis we test the accuracy of the models for correctly predicting whether a given subject under defined ambient conditions feels in comfort or not (i.e., a binary prediction task). As the output of the registered data set (PMV) is continuous and the proposed model is binary, the data set has been discretized, selecting two different possible outputs, *comfort* ($-0.5 < \text{PMV} < 0.5$) or *not comfort* (rest of the values) (in relationship to Fig. 1, *comfort* corresponds to the neutral indicated zone, and *not comfort* to the outside region). The whole data set was divided in training and test data sets, using 60% and 40% of the total cases. The C-Mantec neural network algorithm was run with the following standard configuration for the parameters: $g_{fac} = 0.05$, $I_{max} = 1000$, $\phi = 2$; and two models were considered: one with the standard six input variables used by the theoretical models (Fanger and COMFA) denoted as '6 Var' model, and a second one that also includes as input variables *Age*, *Sex* and the *Body Mass Index* indicated as '9 Var.' model. The results are shown in Table 5 where the first column indicates the used method; the second column shows the accuracy obtained for which the mean value plus standard deviation are indicated ( maximum and minimum values are also shown). The last column indicates the number of neurons that the C-Mantec model automatically choose, and this column also contains three sub-columns with mean plus standard deviation, maximum and minimum values. 100 randomly runs for the indicated data split scheme were performed for each model.

One of the main advantages of using the proposed neural network model is that, as it usually generates architectures with a low number of neurons, a relatively simple

**Table 5** Accuracy values for the prediction of *Comfort Not Comfort* sensation according to the theoretical methods (Fanger and COMFA) and proposed neurocomputational method (C-Mantec)

| Method | Accuracy | | | # of neurons | | |
|---|---|---|---|---|---|---|
| | Mean ± Std | Max | Min | Mean ± Std | Max | Min |
| Fanger | 0.5287 ± 0.0226 | 0.5816 | 0.4645 | – | – | – |
| COMFA | 0.5698 ± 0.0235 | 0.6277 | 0.5248 | – | – | – |
| C-Mantec Model (6 Var) | 0.8335 ± 0.0208 | 0.8723 | 0.7801 | 10.89 ± 1.1538 | 14 | 9 |
| C-Mantec Model (9 Var) | 0.8438 ± 0.0212 | 0.9113 | 0.7872 | 6.17 ± 0.4935 | 7 | 5 |

C-Mantec performance was analyzed using as inputs the usual six variables (6 Var.) and an extended set of variables (9 Var.) (See text for details)

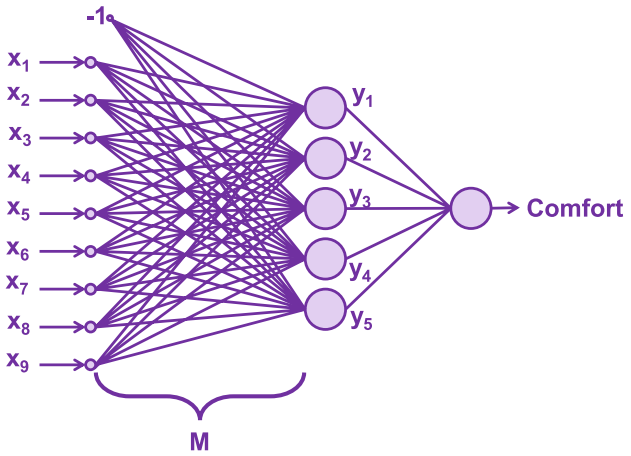


**Fig. 6** Neural network architecture generated by the C-Mantec algorithm for estimating as a function of the 9 input variable whether a human subject is in a Comfort or No Comfort situation

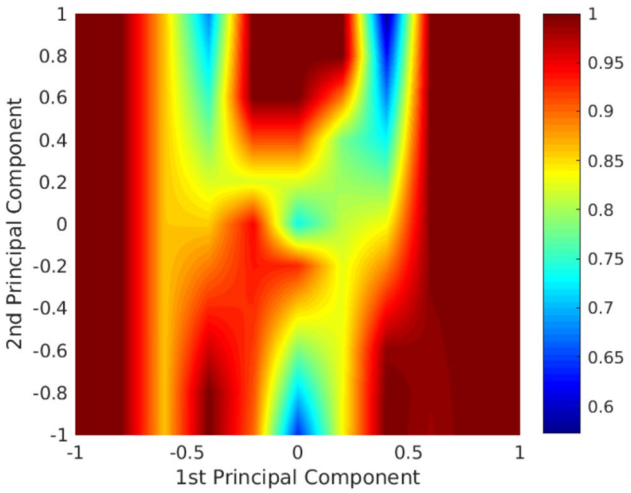


**Fig. 7** Probability of correct decision of the designed neural network system according to the first two Principal components of the input patterns

logical equation can be extracted, that in the present case corresponds to the comfort equation. Equations 10 and 11 show the logical function for the *comfort / not comfort* case in which a model with only 5 neurons in the hidden layer has been chosen in order to simplify the model as much as possible (this model achieves a probability of success of 89.57%). Fig. 6 shows such a network comprising the 9 input neurons (plus the bias term), the synaptic weights matrix M (learnt during training), the 5 hidden layer neurons ($Y_i$) and the single binary output. Eq. 11 represents mathematically the final operation of the shown architecture, with $Y_i$ with $i = 1, \ldots, 5$ values representing the output of the equation 10, obtained through a multiplication between a matrix of the synaptic weights ($M$) of the neural architecture and a vector of inputs ($X_1, X_2, ..., X_9$)(the $-1$ term at the last component of the vector corresponds to a fixed bias term). The nine $X_i$ inputs represent the ambient and subject variables which are Solar Radiation, Humidity, Temperature, Wind, Clothing, Activity, Sex, BMI, and Age, respectively. Thus by multiplying the learned synaptic weights matrix by the ambient and subject variables, the response of 5 intermediate neurons can be obtained, and from these the *Comfort/Not Comfort* condition can be computed using Eq. 11. This equation, representing the output operation of the neural network, computes the majority function of the activation of the neurons of the hidden layer ($Y_i$), such that if three or more of the five factors of the equation are satisfied ($Y_i \leq 0$), then the output variable Comfort is True (and False in any other case, i.e., two or less number of true factors)

In a further analyses aimed to understand the obtained model, we computed the probability of correct decision when the two first principal components of the inputs are considered (see also Fig. 5 and related text in relationship to the PCA). Fig. 7 shows this probability of correct decision of the designed neural network system generated from the analysis of the two first principal components from the raw data: first, the principal component has been obtained for each input pattern of the data set, to then normalize the space of the two principal components between $-1$ and 1. From these values, the probability of correct decision is computed for the whole data set while missing values are computed using a linear interpolation of the rest of the values. It is possible to identify in the graph, three areas where the prediction accuracy is lower than the average (approximately in the range of 0.6). An analysis of the data that corresponds to these three cases shows that: the two areas with values around ($-0.5$, 0.9) and (0.5, 0.9) corresponds to borderline situations between *Warm/Hot* thermal comfort sensation with high radiance levels and for the case of subject of both sexes. The region around the point (0, $-0.9$) corresponds to

**Table 6** Accuracy values for the prediction of perceived comfort sensation in 5 categories according to Fanger, COMFA models and C-Mantec

| Method | Accuracy | | | MSE | | | # of neurons | | |
|---|---|---|---|---|---|---|---|---|---|
| | Mean | Max | Min | Mean | Max | Min | Mean | Max | Min |
| Fanger | 0.420 ± 0.022 | 0.479 | 0.369 | 1.366 ± 0.123 | 1.675 | 1.075 | – | – | – |
| COMFA | 0.244 ± 0.017 | 0.284 | 0.202 | 9.934 ± 0.517 | 10.993 | 8.621 | – | – | – |
| C-Mantec Model(6 Var) | 0.517 ± 0.037 | 0.624 | 0.422 | 1.123 ± 0.248 | 1.394 | 0.892 | 52.2 ± 2.49 | 54 | 48 |
| C-Mantec Model (9 Var) | 0.585 ± 0.048 | 0.678 | 0.453 | 0.805 ± 0.171 | 1.552 | 0.526 | 33.66 ± 1.38 | 38 | 30 |

C-Mantec performance was analyzed using as inputs the usual six variables (6 Var.) and an extended set of variables (9 Var.) (See text for details)

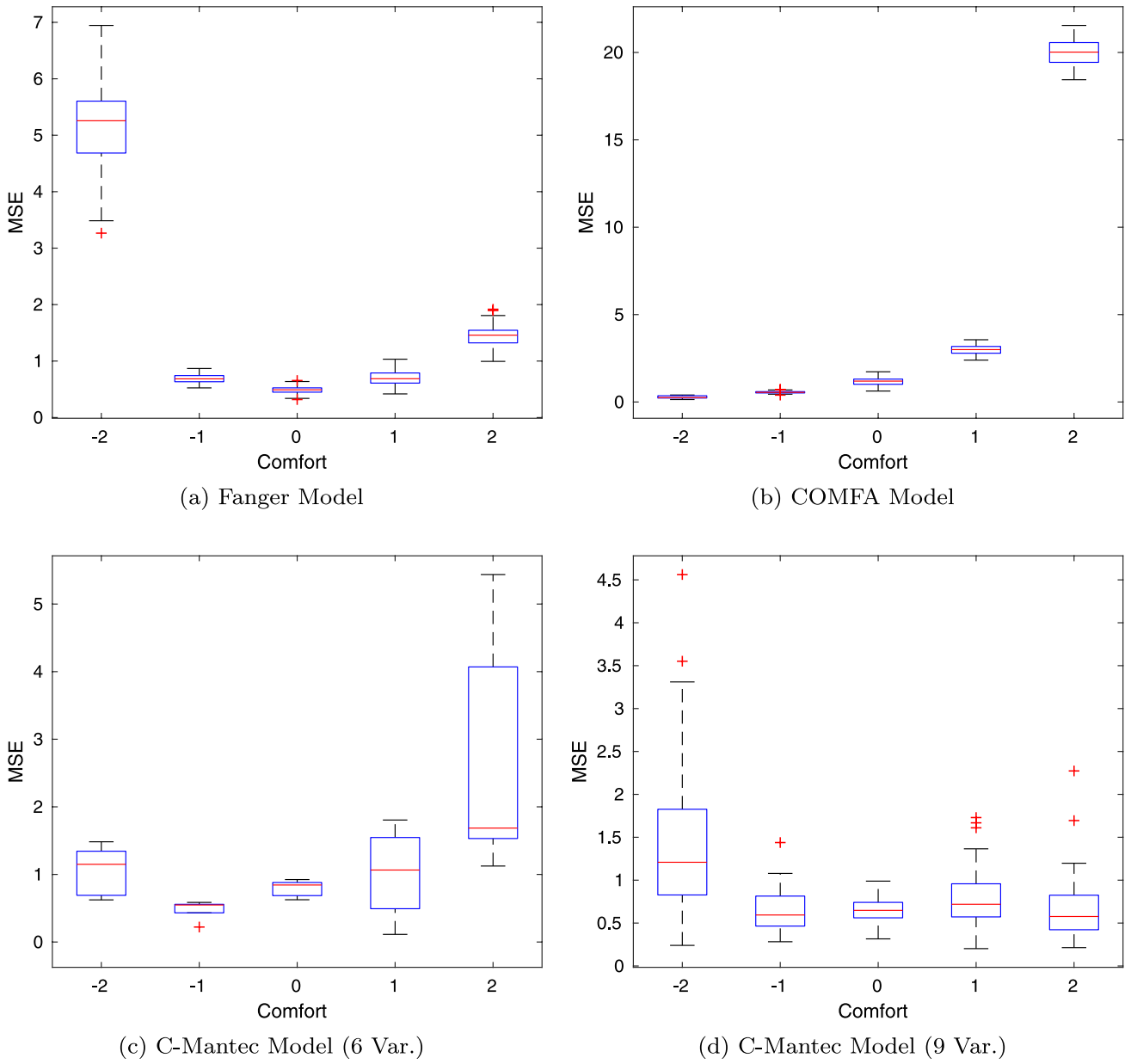


**Fig. 8** MSE distribution for the four used models for the case of predicting thermal comfort in 5 categories (Cold, Cool, Neutral, Warm and Hot). Note that the Y-axis scale is different in each case (see text for more details)

a borderline region between *Cool/Cold* comfort sensation for the case of no radiation.

In the previous analysis we consider only the situation of *Comfort/ Not Comfort*, so we decided to extend the study of the model prediction for the case of a graded thermal sensation, using a discretized range of 5 possible response categories: Cold, Cool, Neutral, Warm and Hot (See Fig. 1 for the range of PMV values and its corresponding PDD values).

Table 6 shows the accuracy and the mean square error perform in the thermal comfort analysis according to the 5 possible output states for the neural network model proposed and for the traditional Fanger and COMFA methods. The obtained prediction values are for all four cases worse than those previously obtained for the binary case, and the reason for this is that correctly predicting the output in 5 categories is a more difficult task. It can be seen that also in this case the neural network outperforms the other two traditional models. The first column in Table 6 shows the method used; second and third column show the accuracy and the MSE respectively, while the last column indicates the number of neurons that the neural network model needs in order to carry out the prediction.

A further analysis was carried out to study how the errors are distributed for each category and for each of the three applied methods, and the results are shown in Fig. 8. On each box, the central mark indicates the median, and the bottom and top edges of the box indicate the $25^{th}$ and $75^{th}$ percentiles, respectively. The whiskers extend to the most extreme data points not considered outliers, and the outliers are plotted individually using the '+' symbol.

## 6 Conclusions

A novel study based on the use of a constructive neural network model for the estimation of thermal comfort has been introduced and applied to new recorded data from several human subjects under different ambient conditions. The constructive method employed generates small architectures that permit to generate a relatively simple equation (Eq. 11) for the estimation of thermal comfort, allowing its implementation in low-cost hardware devices that might be incorporated in HVAC systems for its automatic regulation.

In a first binary prediction task of *Comfort/No Comfort* the neural network model performed quite well with average values above 0.83, outperforming the results from the Fanger and COMFA models. When the prediction task was extended to 5 categories *(Cold, Cool, Neutral, Warm and Hot)*, the accuracy reduced much (maximum values of 0.624) but still the introduced model was quite superior to Fanger and COMFA models, noting that in this case the COMFA model performed much worse than the Fanger one. An analysis carried out on the distribution of MSE shows that the Fanger model leads to very high error values for the *Hot* category, and this indicates that irradiance estimation is not accurately performed. The analysis for the Fanger and ANN models also show a bias with larger than average errors but in this case for the *COLD* category. Fanger model does not take into account radiation conditions, and this might explain part of the bias.

Neural network models were trained with standard 6 environment variables and also adding other 3 subject-related variables (age, sex and BMI). The addition of these three variables leads to a $1.23\%$ and $13.15\%$ improvement in the binary and 5-category prediction cases respectively, also observing the fact that the 9 input variables model needed a lower number of neurons in both cases, indicating that this extra information reduces the complexity of the task.

The overall conclusion of the present work is that neural network-based models seem adequate for the estimation of thermal comfort perception, leading to more accurate prediction values than standard Fanger and COMFA models. Nevertheless, the low prediction accuracy values (in the range of 0.5-0.6) for the 5 categories case might indicate that further subject or ambient conditions should be taken into account in order to increase these levels, and in this sense, it is clear that radiation is a key factor to take into account in further analysis.

**Acknowledgements** The authors acknowledge the support from MINECO (Spain) through grants TIN2017-88728-C2-1-R and PID2020-116898RB-I00 (MICINN), and from Junta de Andalucía through grant P10-TIC-5770 and from Junta de Andalucía and Universidad de Málaga through grant UMA20-FEDERJA-045 (all including FEDER funds).

**Funding** The authors have not disclosed any funding.

**Data availability** Enquiries about data availability should be directed to the authors.

## Declarations

**Conflict of interest** Francisco Ortega-Zamorano, José M. Jerez, José Rodríguez-Alabarce, Kusha Goreishi, Leonardo Franco declare that they have no conflict of interest.

**Ethical approval** All procedures performed in studies involving human participants were in accordance with the ethical standards of the institutional and/or national research committee and with the 1964 Helsinki declaration and its later amendments or comparable ethical standards. This article does not contain any studies with animals performed by any of the authors.

**Informed consent** Informed consent was obtained from all individual participants included in the study.

## References

Acquaah YT, Gokaraju B, Tesioro RC III, Monty G, Roy K (2023) Occupancy and thermal preference-based hvac control strategy using multisensor network. IEEE Sensors Journal 23(11):11785–11795

Alghamdi S, Tang W, Kanjanabootra S, Alterman D (2022) Effect of architectural building design parameters on thermal comfort and energy consumption in higher education buildings. Buildings 12(3):329

Ashrae: ANSI/ASHRAE Standard 55-2010 (2010) Thermal Environmental Conditions for Human Occupancy. American Society of Heating, Air-Conditioning, and Refrigeration Engineers, Inc.

Bindu NP, Sastry PN (2023) Automated brain tumor detection and segmentation using modified unet and resnet model. Soft Computing 27(13):9179–9189

Brown R, Gillespie T (1986) Estimating outdoor thermal comfort using a cylindrical radiation thermometer and an energy budget model. International Journal on Biometeorology 30:43–52

Castilla M, Álvarez J, Ortega M, Arahal M (2013) Neural network and polynomial approximated thermal comfort models for hvac systems. Building and Environment 59:107–115

Chen B, Lian Y, Xu L, Deng Z, Zhao F, Zhang H, Liu S (2024) State-of-the-art thermal comfort models for car cabin environment. Building and Environment 262:111825

Fanger P (1967) Calculation of thermal comfort: Introduction of a basic comfort equation. ASHRAE Transactions 73:1–20

Feng C, Ma F, Wang R, Li W, Gao J (2023) A thermal comfort evaluation on vehicular environments based on local human body thermal sensations. Results in Engineering 17:100907
Ferreira P, Ruano A, Silva S, Conceicao E (2012) Neural networks based predictive control for thermal comfort and energy savings in public buildings. Energy and Buildings 55:238–251
Franco L, Elizondo D, Jerez J (2010) Constructive neural networks. Springer, Berlin, Germany
Frean M (1990) The upstart algorithm: a method for constructing and training feedforward neural networks. Neural Computation 2(2):198–209
Ganaie MA, Hu M, Malik AK, Tanveer M, Suganthan PN (2022) Ensemble deep learning: A review. Engineering Applications of Artificial Intelligence 115
Gómez I, Mesa H, Ortega-Zamorano F, Jerez-Aragonés J, Franco L (2020) Improving learning and generalization capabilities of the c-mantec constructive neural network algorithm. Neural Computing and Applications 32(13):8955–8963. https://doi.org/10.1007/s00521-019-04388-2
Haykin S (1998) Neural Networks: A Comprehensive Foundation, 2nd edn. Prentice Hall PTR, Upper Saddle River, NJ, USA
Iman M, Arabnia HR, Rasheed K (2023) A review of deep transfer learning and recent advancements. Technologies 11(2):40
Kenny N, Warland J, Brown R, Gillespie T (2009) Part a: Assessing the performance of the comfa outdoor thermal comfort model on subjects performing physical activity. International Journal of Biometeorology 53(5):415–428
Kenny N, Warland J, Brown R, Gillespie T (2009) Part b: Revisions to the comfa outdoor thermal comfort model for application to subjects performing physical activity. International Journal of Biometeorology 53(5):429–441
Kisel'ak J, Lu Y, Svihra J, Szepe P, Stehlik M (2021) "spocu": scaled polynomial constant unit activation function. Neural Computing & Applications 33(8):3385–3401
LeCun Y, Bengio Y, Hinton G (2015) Deep learning. Nature 521:436–444
Lindberg F, Grimmond C, Gabey A, Huang B, Kent C, Sun T, Theeuwes N, Järvi L, Ward H, Capel-Timms I, Chang Y, Jonsson P, Krave N, Liu D, Meyer D, Olofson K, Tan J, Wästberg D, Xue L, Zhang Z (2018) Urban multi-scale environmental predictor (umep): An integrated tool for city-based climate services. Environmental Modelling and Software 99:70–87
Liu Z, Li J, Xi T (2023) A review of thermal comfort evaluation and improvement in urban outdoor spaces. Buildings 13(12):3050
Lopez EG, Heard C (2023) Social acceptance of a thermal architectural implementation proposal. Sustainability 15(5):4121
López-Rubio E, Ortega-Zamorano F, Domínguez E, Muñoz Pérez J (2019) Piecewise polynomial activation functions for feedforward neural networks. Neural Processing Letters 50(1):121–147
Mehrotra K, Mohan CK, Ranka S (1997) Elements of Artificial Neural Networks. MIT Press, Cambridge, MA, USA
Michael K, Garcia-Souto M, Dabnichki P (2017) An investigation of the suitability of artificial neural networks for the prediction of core and local skin temperatures when trained with a large and gender-balanced database. Applied Soft Computing Journal 50:327–343
Moreno-Sáez R, Mora-López L (2014) Modelling the distribution of solar spectral irradiance using data mining techniques. Environmental Modelling and Software 53:163–172
Nam C, Lierhammer L, Buntemeyer L, Evadzi P, Cabana D, Celliers L (2024) Changes in universal thermal climate index from regional climate model projections over european beaches. Climate Services 34:100447
Olesen B, Parsons K (2002) Introduction to thermal comfort standards and to the proposed new version of en iso 7730. Energy and Buildings 34(6):537–548
Ono E, Mihara K, Lam KP, Chong A (2022) The effects of a mismatch between thermal comfort modeling and hvac controls from an occupancy perspective. Building and Environment 220:109255
Ortega-Zamorano F, Jerez J, Subirats J, Molina I, Franco L (2014) Smart sensor/actuator node reprogramming in changing environments using a neural network model. Engineering Applications of Artificial Intelligence 30:179–188
Pallubinsky H, Kramer RP, Lichtenbelt WDvM (2023) Establishing resilience in times of climate change-a perspective on humans and buildings. Climatic Change 176(10)
Pilliza G, Roman O, Morejon W, Hidalgo S, Ortega-Zamorano F (2018) Risk analysis of the stock market by means self-organizing maps model
Reed RD, Marks RJ (1998) Neural Smithing: Supervised Learning in Feedforward Artificial Neural Networks. MIT Press, Cambridge, MA, USA
Rodríguez-Alabarce J, Ortega-Zamorano F, Jerez JM, Ghoreishi K, Franco L (2016) Thermal comfort estimation using a neurocomputational model. In: 2016 IEEE Latin American Conference on Computational Intelligence (LA-CCI), pp 1–5
Sangkertadi S, Syafriny R (2014) New equation for estimating outdoor thermal comfort in humid-tropical environment. European Journal of Sustainable Development 3:43–52
Subirats J, Franco L, Jerez J (2012) C-mantec: A novel constructive neural network algorithm incorporating competition between neurons. Neural Networks 26:130–140
Torres-Molina R, Guachi-Guachi L, Guachi R, Stefania P, Ortega-Zamorano F (2020) Learning style identification by chaea junior questionnaire and artificial neural network method: A case study. Advances in Intelligent Systems and Computing 1067:326–336
Zadmirzaei M, Hasanzadeh F, Susaeta A, Gutierrez E (2024) A novel integrated fuzzy dea-artificial intelligence approach for assessing environmental efficiency and predicting [CDATA[co_2]]$co_2$ emissions. Soft Computing 28(1):565–591